

Use of Early Effect Biomarker Data to Enhance Dose-Response Models of Lung Tumors in Rats Exposed to Titanium Dioxide

Bruce Allen¹, Andrew Maier², Alison Willis², Lynne T. Haber^{2*}

¹Bruce Allen Consulting

²Toxicology Excellence for Risk Assessment (*TERA*), Cincinnati, Ohio 45211

***Corresponding author**

Lynne Haber

Toxicology Excellence for Risk Assessment

2300 Montana Ave., Suite 409

Cincinnati, OH 45157

Phone: 513-542-7475 x17

Fax: 513-542-7487

Email: haber@tera.org

ABSTRACT

The use of precursor data in risk assessments is being increasingly emphasized as the future of toxicology. Due to the limited validation and the lack of vetted approaches for quantitatively incorporating biomarker data into dose-response assessments, current uses of biomarker data are usually constrained to hazard characterization. This paper presents a biologically-informed empirical dose-response modeling approach that incorporates biomarker data and lung tumor response in rats exposed to titanium dioxide (TiO₂). The models are a series of linked “cause-effect” functions describing the relationships between successive key events, including the ultimate tumor response. This approach was used to evaluate hypothesized pathways for biomarker progression from lung burden through several intermediate potential biomarkers of effect (polymorphonuclear lymphocyte count indicative of inflammation, proteins in bronchoalveolar lavage fluid indicative of respiratory tract epithelium damage, pulmonary fibrosis incidence, and alveolar cell proliferation), to the tumor endpoint. When the model allowed both fibrosis and cell proliferation to predict the tumor response, the cell proliferation data provided no additional predictive power beyond that of the fibrosis response. The likelihood maximization approach allowed the calculation of a lung burden-based benchmark dose for lung tumors that directly incorporated data for biomarkers of exposure and effect. Although enhancements to the model are needed before it or similar models can be used for regulatory purposes, the biomarker-based modeling approach demonstrated for TiO₂ as a case study provides more-refined dose-response estimation than that obtained using the traditional approach of dose-response modeling based only on administered dose and clinical endpoint data.

1.0 INTRODUCTION

Biomarkers have long been considered as indicators of exposure, toxicity, and susceptibility (NAS/NRC, 1989). The recent NAS report on Toxicity Testing in the 21st Century (NAS/NRC, 2007) has increased attention on the use of biomarkers in a quantitative risk assessment context, particularly biomarkers of early effect obtained from *in vitro* high-throughput studies. Regardless of type of biomarker, lack of validation has continued to be a key barrier to increased biomarker application in human health risk assessment (Maier et al., 2004). Thus a goal of this current work is to validate early effect biomarkers and to connect them to the precursor events indicating perturbations from homeostasis that are predictive of clinical disease. One important step in that direction is the development of a suite of methods to quantitatively connect biomarker data to established clinical endpoints, such as tumors. In earlier work, we used a suite of validation approaches for evaluating exposure and effect biomarkers for benzene-induced acute myeloid leukemia (AML) (Haber et al., 2010; Hack et al., 2010) (www.tera.org/pubs). In particular, a Bayesian network model was used to evaluate and compare individual biomarkers and quantitatively link the biomarker data along the exposure-disease continuum and with the ultimate tumor endpoint. This paper builds on that earlier work, by presenting a proof-of-concept case study for the use of biomarker data to quantitatively link inhalation exposure to titanium dioxide (TiO₂) with lung tumors using an alternative dose-response modeling approach. While a number of enhancements would be needed prior to the use of this modeling or the results for regulatory purposes, this paper illustrates an approach for using a series of linked “cause-effect” functions to describe the relationships between successive key events and the ultimate tumor response. This illustrates an approach intermediate between the use of default methods and the labor- and data-intensive approach needed to develop and parameterize a biologically-based dose-response model.

Titanium dioxide (TiO₂) is a commercially important white pigment for paints and dyes and is used in a variety of consumer products (NIOSH 2005). Epidemiology and toxicology studies have been conducted to evaluate the ability of TiO₂ to induce respiratory tract diseases. Additional toxicological investigations were spurred by the interest in examining the impacts of very small particle size on the ability of relatively nonreactive materials to induce lung toxicity. TiO₂ exposure is described in the available health effects studies based on its differing forms (rutile or anatase) and its particle size range. Materials containing particles ranging from 0.1 to 10 μm are considered “fine” and those containing particles less than 0.1 μm are described as “ultrafine”.

Several epidemiological studies of workers exposed to TiO₂ found little evidence of increased lung cancer mortality or morbidity (reviewed in NIOSH 2005). Chen and Fayerweather (1988) found no significant association between TiO₂ exposure and pulmonary disease, lung cancer, or fibrosis in a nested case-control study of 2,477 male workers (1,576 exposed) from two TiO₂ production plants from 1935-1983 (quantitative exposure data were not collected). Similarly, no effect on total cancers, lung cancer, or other causes of death was seen by Fryzek et al. (2003) in an evaluation of 4,241 workers employed for six months or more from 1960-2000 in four production plants in the US.

Total mean TiO₂ dust levels were reported as reaching as high as 13.7 mg/m³ in earlier years and as low as 3.1 mg/m³ in more recent years. In a re-evaluation of lung cancer risk from a population-based case-control study of 293 substances, Boffetta et al. (2001) found no significant association between lung cancer risk and TiO₂ exposure. Boffetta et al. (2004) conducted a retrospective cohort mortality study of 15,017 workers in six European countries who had been employed in TiO₂ manufacturing factories for at least one month. Although the authors found an increased risk of lung cancer mortality in males (SMR = 1.23; 95% CI = 1.10-1.38), there was no evidence of a dose-response relationship between increasing TiO₂ concentration and lung cancer; the authors noted that the study may have lacked the statistical power to detect a dose-response.

In contrast to the generally negative occupational data, TiO₂ has been observed to cause lung cancer in rats. Lee et al. (1985) exposed 200 rats (CD, Sprague-Dawley derived) to 0, 10, 50, or 250 mg/m³ fine, rutile TiO₂ for 6 hr/day, 5 days/week for 2 years. Particle size was reported as 1.5-1.7 micrometers (µm) mass median aerodynamic diameter (MMAD). Bronchioalveolar adenomas and squamous cell carcinomas (SCCs) were reported at 250 mg/m³. Muhle et al. (1991) used exposure to 5 mg/m³ fine TiO₂ (77% respirable) as a control in a study of Fischer 344 rats exposed to toner for up to 24 months, and found no increase in tumor incidence in the TiO₂ exposed animals. Heinrich et al. (1995) exposed 100 Wistar rats and NMRI mice to ultrafine anatase TiO₂ at 10 mg/m³ concentration for 2 years. The primary particle size was reported as 15 to 40 nanometers (nm), but the particles agglomerated, so the actual MMAD was 0.8 µm. Mice suffered a significantly reduced lifespan with no tumors; however high control rates of tumors may have decreased the ability to detect significant carcinogenic effects. In the rats, lung adenocarcinomas were statistically increased, and 20 rats developed benign keratinizing cystic squamous cell tumors of the respiratory tract. These tumors were later recharacterized as proliferative keratinizing cysts, a lesion of questionable pathological significance to humans (Boorman et al., 1996; Fryzek et al., 2002; Dankovic et al., 2007); therefore these tumors were excluded from the analysis described in this paper. Similarly, re-evaluations of the SCCs in the Lee et al. (1985) study have determined that these lesions were mostly keratinizing cysts (Warheit and Frame, 2006), and so the SCCs in that study were excluded from our analysis as well.

A key consideration in a quantitative risk assessment for cancer is the mode of action (MOA). MOA is of particular importance for the current assessment, due to the direct relationship between identification of the MOA and identification of precursors or effect biomarkers that might be related to carcinogenesis. Of the three tumor studies, only the Muhle et al. (1991) study presented data on precursor effects (aside from fibrosis incidence) useful for a biomarker-based assessment, and that study tested only one dose. However, the literature does contain other studies with more complete information on dose response for precursors that were considered in evaluation of potential biomarkers of effect.

Limited data are available regarding the genotoxic effects of TiO₂. As reviewed by IARC (1989), TiO₂ was negative in the only gene mutation studies available, conducted in *Salmonella typhimurium* and *Escherichia coli*. Negative results were also

observed in a DNA damage assay (cell killing in DNA-repair deficient *Bacillus subtilis*) and in a Syrian hamster embryo (SHE) cell transformation assay, which evaluates multiple aspects of the carcinogenic process. As noted by NIOSH (2005), positive results have been observed for micronuclei in Chinese hamster ovary (CHO) cells (a measure of chromosome-level damage). Other evidence of TiO₂-induced DNA damage includes positive results for sister chromatid exchanges in CHO cells, and for apoptosis in SHE cells (apoptosis can result from multiple causes, including DNA damage). These results are consistent with the conclusion that TiO₂ can cause DNA damage, but not via a direct DNA-reactive mechanism.

In light of the low direct DNA reactivity of TiO₂ and other low-toxicity poorly soluble particles, it has been hypothesized that particle accumulation and the resulting inflammation play a causal role in the development of rat lung tumors following inhalation exposure (reviewed by Dankovic et al., 2007; Elder et al., 2005; ILSI, 2000). Reactive oxygen species (ROS) may be involved both in the initial regulation of the inflammatory process and as a cause of cytotoxicity and secondary gene mutations. Together with epithelial proliferation that is likely to result from inflammation, the secondary genotoxicity can favor tumor formation or progression. This hypothesis is supported by the correlation of species susceptibility to lung tumors with precursors of inflammation, ROS, histopathology, and oxidative DNA damage. For example, mice exposed to TiO₂ via instillation showed no evidence of inflammation (Hubbard et al., 2002) and TiO₂ does not cause lung tumors in mice. While this correlation held in this case, it does not hold in the broader scenario – some chemicals cause lung inflammation without causing lung tumors, and some chemicals cause lung tumors without causing inflammation. However, lack of specificity is considered one of the less impactful considerations in evaluating a MOA hypothesis (US EPA, 2005). The absence of evidence for direct mutagenicity for TiO₂ also does not rule out the potential for some contribution from other causes of genotoxicity in the overall MOA. Since precursor key events that might be associated with downstream genotoxicity mechanisms (e.g., inflammation and ROS generation) are incorporated into the analysis, some of these potential underlying DNA-related mechanisms may at least in part be accounted for in the resulting model.

Figure 1 lays out the key steps in the inflammatory MOA. The primary pathway shown focuses on the sequential and experimentally-observed intermediate steps that were amenable to modeling. The dashed pathway from fibrosis to tumors represents a hypothesized pathway that has not been fully confirmed as being separate from the cell proliferation step. The dotted pathways from lung burden reflect the presence of mechanistic steps (associative events or modulating factors) that are important for the MOA, and which may impact multiple steps of the “primary” pathway (indicated by the solid arrows), but for which there were no TiO₂ data. Specifically, because ROS and cytotoxicity are likely to play important and perhaps multi-faceted roles in the MOA, but data were not available to include these endpoints in the model, the model also included connections directly between the lung burden and all later steps in the “primary” pathway (except fibrosis and cancer), as a way of accounting for other influences that do not progress through the order of the primary pathway as shown. As noted in the discussion,

incorporation of data from other low-toxicity poorly soluble particles, in subsequent follow-up analyses, may allow these other steps to be incorporated into the model.

Determination of the appropriate dose metric is a key consideration in quantitative modeling of particle dose-response. Oberdorster et al. (1994, 1996) found that surface area of particles is a predictor of inflammatory response for ultrafine particles. Primary experimental evidence supporting surface area as a predictor of inflammatory response comes from the work of Driscoll (1996) and Lison et al. (1997). The appropriateness of surface area as a dose metric for fine and ultrafine particles was supported by the analysis of Dankovic et al. (2007), who found that surface area was a good predictor of the inflammatory response (as measured by polymorphonuclear lymphocyte [PMN] count) or tumor response following exposures to several low toxicity poorly soluble particles. In a reanalysis of the Oberdorster et al. (1994) data, Moss and Wong (2006) described a further enhancement of this focus on surface area, recommending a dose metric of square centimeters of particle projected area per square centimeter of exposed macrophage surface, suggesting that this metric reflects the degree to which the macrophage surface is shielded from other objects. Based on these considerations, our analysis used particle surface area as the dose metric. The metric was normalized by lung weight, to account for differences in lung size among rat strains, and as an appropriate species-normalized approach for extrapolating to humans.

Based on these considerations, this paper investigated an approach for quantitatively incorporating the precursor biomarker data into the dose-response prediction for carcinogenesis, using rat lung tumors induced by inhalation exposure to TiO₂ as a case study. Information on the steps in the pathogenic process was used to identify and order key events (and associated biomarkers) to include in the modeling. The case study was developed to demonstrate a possible approach that could be more fully developed for using biomarker data to inform dose-response behavior in the absence of knowledge to build a validated BBDR model.

2.0 METHODS

2.1 Specification of Cascade of Events

The initial step in formulating and quantitatively representing the relationship between TiO₂ exposure and lung cancer development in rats was the specification of a sequence, or progression, of events that linked such exposure to the occurrence of the tumorigenic responses observed in that species. Figure 1 shows the progression that was the basis for this investigation. As mentioned previously, connections between lung burden and the precursors reflecting loss of integrity of the blood:air barrier (e.g., lactate dehydrogenase [LDH] or protein in the bronchoalveolar lavage fluid [BALF]) and cell proliferation (bromodeoxyuridine [BrdU]) were included to represent the potentially important roles played by ROS and cytotoxicity, which are assumed to be consequences of (and quantitatively related to the level of) lung burden. Data were not available to include the ROS and cytotoxicity endpoints directly in the model. The use of lung

burden directly as a surrogate for ROS and cytotoxicity implicitly assumes that ROS and cytotoxicity responses are proportional (linearly related) to lung burden.

2.2 Identification and Selection of Studies and Endpoints

A literature search was conducted to identify studies that might provide information about the consequences of TiO₂ inhalation exposure and endpoints related to the pathophysiological progression laid out in Figure 1. Since TiO₂-induced tumors have been seen only in rats, data collection for potential tumor precursors was also focused on rats. Initially, exposures other than inhalation (e.g., from instillation studies) were considered, but these studies were not used due to different patterns of particle deposition following inhalation and instillation exposure. *In vitro* studies were also excluded, due to uncertainties in converting *in vitro* doses to units of lung burden. Table 1 presents the data extracted from the studies and used in the modeling.

The studies ultimately selected for analysis had to provide the following information. First, there had to be enough data to estimate the lung burden in the appropriate dose metric (in m² TiO₂/g lung tissue) associated with the inhalation exposure groups. As described in the Introduction, lung burden measured in terms of surface area of TiO₂ per gram of lung tissue was considered to be the best available dose metric for describing the relationship between inhalation exposure to TiO₂ and toxic effects, although other metrics have been proposed. Typically, the requirement for data in this dose metric meant that, in addition to measurements of the mass of TiO₂ in the lung, study-specific values for specific surface area (m² per g TiO₂) were reported or could be assumed, as well as some information about lung weight (or body weight from which lung weight could be computed). From these data, the desired dose metric was calculated as (μg TiO₂/g lung)*(m² TiO₂ surface area/g TiO₂) or (μg TiO₂/lung)*(m² TiO₂ surface area/g TiO₂)/(g lung). Table 2 shows the basis for the lung burden calculations for the studies selected for analysis.

The second piece of required information was that the reported results for one or more endpoints needed to include sufficient data to allow likelihood calculations (see below). For a continuous endpoint, that entailed the reporting of the sample size, the mean, and the standard deviation (or a value, such as standard error, from which standard deviation could be derived). For a dichotomous endpoint, that entailed the reporting of the sample size and number affected.

The last column of Table 2 indicates the endpoints that were ultimately included in the analysis for each study. Table 3 provides all of the endpoints considered, including those selected for the analysis, by the type of event that they characterized; the types of events of interest were those represented in the progression in Figure 1. Thus, for example, the PMN endpoint was one of those that were considered (and ultimately selected) to characterize the event of inflammatory response. The endpoints selected were considered superior to the others primarily because they were reported with adequate data for more studies or because the dose-response pattern (across studies) was

more consistent (e.g., the normalized results tended to be more monotonically related to lung burden).

2.3 Data Representation

For each of the three precursors, PMN, LDH, and BrdU, the precursor response has been “normalized” to enhance consistency with respect to the measurement of each endpoint across studies. Such normalization reduces study-dependence, for example by eliminating systematic differences in measurement or reporting that might occur across laboratories, and it also facilitates the combination of observations that may have been reported in different formats (e.g., as percent of control from one study but with mean values in another study).

Within each study, z-score normalization was done (Larsen and Marx, 2000). For a precursor, p_j , with reported means m_0, m_1, \dots, m_G , and standard deviations s_0, s_1, \dots, s_G for the control group and the exposure groups 1 through G in a study, respectively, the normalized values used in the analysis are

$$\begin{aligned} m'_i &= (m_i - m_0) / s_0, \\ s'_i &= s_i / s_0 \end{aligned} \quad \text{Eq. 1}$$

for i from 0 to G. Note that for every precursor from every study, $m'_0 = 0$ and $s'_0 = 1$. In the analyses described below, it is assumed that these normalized precursor observations are normally distributed. The dose-response relationships used in those analyses, describing the relationship between lung burden and normalized precursor values have been set so that the intercepts of those relationships are 0.

2.4 Likelihood-Based Approach

For each of the three continuous precursors under consideration (PMN, LDH, and BrdU labeling), all of the normalized data from across the studies reporting the relationship between lung burden and the precursor values were pooled and plotted (Figure 2a). The overall patterns of the response relative to lung burden were examined. A power function was determined to provide a reasonable representation of the overall patterns seen; such a function was used for all the subsequent dose-response analyses of the continuous endpoints. This pre-selection of a dose-response function was an expedient assumption, as a way to limit the scope of the likelihood maximization problem, and a reasonable first step in the overall process of likelihood-based estimation described below, because the power function was apparently flexible enough to provide an adequate description of the dose-response relationships in the selected TiO_2 data set. Additional comments concerning this initial step are included in the Discussion section below.

The functional relationship between lung burden, b , and PMN was therefore represented as

$$p = \alpha_1 * b^{\beta_1}, \quad \text{Eq. 2}$$

where p represents the normalized values for PMN across all of the studies considered. In accordance with Figure 1, the remaining relationships among the continuous precursors were represented as follows:

$$l = \alpha_2 * p^{\beta_2} + \gamma_2 * b^{\delta_2} \quad \text{Eq. 3}$$

$$a = \alpha_3 * l^{\beta_3} + \gamma_3 * b^{\delta_3} \quad \text{Eq. 4}$$

where l is the normalized LDH response and a is the normalized alveolar BrdU index response. All the α , β , γ , and δ parameters were estimated as discussed further below.

Fibrosis response rate was considered to be a function of only the precursor ‘ l ’, so the probability of a fibrotic response was modeled using a one-hit model:

$$P(f) = 1 - \exp\{-\eta(j) - \theta * l\}, \quad \text{Eq. 5}$$

where the parameters to be estimated were $\eta(j)$, the study-specific background parameters (for $j = 1, 2, 3$ corresponding to the three studies that reported fibrosis rates; see Table 2), and θ , a coefficient for the normalized LDH response that was assumed to be constant across studies. The inclusion of the study-specific $\eta(j)$ parameters was the way in which “normalization” was accomplished for this dichotomous endpoint, the reported rates of which might have been affected by differences among the three experiments (e.g., between males and females in the Lee et al., 1985, study).

Finally, the probability of tumors was modeled using the logistic equation:

$$\text{logit}(P(t)) = \phi_0 + \phi_1 * ER(f) + \phi_2 * a, \quad \text{Eq. 6}$$

where $ER(f)$ was the extra risk of fibrosis. Using extra risk of fibrosis as the predictor variable for tumor probability yields a relationship that is study-independent; extra risk calculated from the one-hit model for fibrosis can be shown to equal $1 - \exp\{-\theta * l\}$, thus eliminating the study-specific parameters. The normalized BrdU labeling endpoint, ‘ a ’ in equation 6, represents the possible effect of proliferation on the probability of tumor, and is already study-independent. The normalization was performed to eliminate the need for study-specific parameters and none were included in the model for the precursor ‘ a ’ endpoint (Eq. 4). Thus, Eq. 6 provides a description of the rates of tumor that is also study-independent.

The estimation of the parameters of equations 2 through 6 was carried out by maximization of the likelihoods associated with the observed data and the models of equations 2-6. This approach obviates the need to have any specific study that measured and reported both cell proliferation (represented by variable ‘ a ’ in the above equations) and fibrosis incidence, for example. In a study reporting fibrosis rates, the modeling uses the “imputed” normalized LDH response associated with the measured lung burden from

that study as the independent variable in equation 5, along with its reported fibrosis rates. “Imputation” of values is accomplished by following the chain of equations back to lung burden, ‘b’, in this example getting imputed values of ‘l’ from equation 3, which in turn requires imputed values of ‘p’ from equation 2.

More specifically, the following procedure was followed for estimation. The parameters for equation 2 were estimated by maximizing the likelihood of the observations of p from all the studies reporting values of PMN. The likelihood was defined assuming that the normalized responses were normally distributed with a mean value determined by lung burden and equation 2. The variances for each group were considered to be independent (one variance parameter was estimated for each group). An Excel spreadsheet was used to define and optimize (maximize) the likelihoods. All of the likelihoods discussed below for the continuous endpoints were based on a normal distribution assumption with independent (group-specific) variances.

Given the maximum likelihood estimates (MLEs) for equation 2, imputed values for p in equation 3 were calculated. Then the maximum likelihood approach was applied again to equation 3, considering the parameters of equation 2 to be fixed at their MLE values. This approach was repeated for equations 4, 5 and 6. In the case of the dichotomous endpoints (fibrosis and tumors), the likelihood was based on an assumption of independent binomial responses within each dose group.

This approach was followed to examine whether simplifications of equations 3, 4, and 6 adequately fit the data (compared to their full forms). For equations 3 and 4, the simplifications considered consisted of dropping the terms using lung burden, b. For equation 6, we examined the possibility that P(t) did not depend on either ER(f) or on the precursor ‘a’, given the presence of the other term.

Once determinations of the final forms of the equations 3 through 6 were made as described above, the chosen forms were used in an “overall” likelihood calculation. That is, when considering the entire ensemble of data (lung burdens, PMN responses, LDH, responses, etc., up to and including the tumor responses) one can calculate the simultaneous likelihood of observing that ensemble, rather than sequentially maximizing the likelihood for discrete segments of the progression and treating the earlier estimates as fixed. Thus, the total log-likelihood being maximized can be expressed as

$$LL = LL_p + LL_l + LL_a + LL_f + LL_t, \quad \text{Eq. 7}$$

where, LL_p is the log-likelihood for the pooled data on normalized PMN, and so on. Of note is that it is the sum of the log-likelihoods that is being maximized and that all of the parameters of equations 2 through 6 are being allowed to vary at the same time. This approach might result in a lower likelihood for one of the components, say LL_a , compared to what would have been estimated by considering that likelihood alone (fixing any parameter values in the earlier equations), but if that decrease is offset by an increase in the likelihood for another component in the sum, say LL_f , then the parameters estimated this way give a better representation of the entire set of data. An Excel

spreadsheet using the “Solver” function was used for this overall likelihood maximization, with starting values for the parameters set equal to those determined in the sequential fitting procedure described above.

3.0 RESULTS

This proof-of-concept analysis used likelihood maximization approaches to estimate the quantitative “cause-effect” relationships among TiO₂ lung burdens, precursor events, and lung tumors following inhalation exposures of rats to TiO₂. *In vitro* studies of precursors were excluded due to difficulties in converting to the dose metric considered most predictive of *in vivo* toxicity (m² TiO₂/g lung tissue). The entire set of original and normalized data points used in this analysis is shown by study in Appendix A.

The log-likelihood estimates derived for the different approaches (Table 4) can be compared to indicate how much difference (in terms of fit to the data) was achieved by each of the approaches. The “sequential” analysis shows the maximized likelihoods for each progression from one precursor to the other, where the maximization for a given stage is dependent on the maximization obtained for every previous stage. The overall likelihood varies all of the parameters simultaneously and maximizes the sum of the log-likelihood components (as opposed to maximization of the component parts one at a time and in order, which is what the sequential approach does). The overall maximization achieved a somewhat better overall likelihood. As can be seen in Table 4, that better overall likelihood reflected improvements of the fit for some linkages, lessened by slightly worse fit for other linkages. The fit was slightly worse (log-likelihood values that were slightly less) for the relationship between PMN and lung burden and for the relationship between LDH and PMN. Conversely, the log-likelihoods for the relationship between LDH and fibrosis and for the relationship between fibrosis and tumors were somewhat greater (because those relationships now had slightly adjusted “independent” variables being used in those two dose-response functions). The difference between the sums of the likelihoods for the sequential approach and for the overall approach was not large; from a “goodness-of-fit” perspective, there would be little visual difference.

The baseline log-likelihoods shown in Table 4 are the maximally parameterized (saturated) likelihoods achieved when no dose-response model is fit (i.e., when each dose group is considered separately and independently from all other dose groups). Such a baseline is an idealized limit on what a maximum likelihood could achieve. It does not, for example, account for the fact that the dose-response functions of interest are monotonic; if the data are nonmonotonic, the baseline likelihood basically ignores such data “quirks” because it does not even consider an explanatory variable such as dose. Nevertheless, a model-achieved maximum log-likelihood is sometimes compared to the baseline (saturated model) maximum log-likelihood to determine how well a model fits. We have not pursued such goodness-of-fit issues here.

All of the model-based likelihoods (sequential and overall) shown in Table 4 are for the versions of the models (equations 3, 4, and 6) stripped of any terms that did not

add to the likelihood when the sequential fitting was done. The parameter estimates obtained for the sequential fitting procedure are shown in Table 5. Thus, for predicting LDH, a separate term corresponding to a direct effect of lung burden on LDH (above and beyond the effect mediated through PMNs) was not required ($\gamma_2 = 0$). Similarly, for the alveolar BrdU index representing cell proliferation, no direct effect of lung burden was required above and beyond the effect mediated through LDH (and hence through PMN to lung burden). Perhaps of greater interest is the observation that fibrosis (as predicted from lung burden through PMNs and LDH) could predict tumor incidence without an additional term corresponding to cell proliferation. (The full model corresponds to Eq. 6.) In other words, there was no added predictive power when the cell proliferation endpoint was added to the logistic equation (Eq. 6) for tumor rate ($\phi_2 = 0$). Even with starting parameter values reflecting a hypothesis that tumor incidence could be fully explained by cell proliferation, maximizing the likelihood resulted in $\phi_2 = 0$, and the tumor incidence predicted by fibrosis and its precursors. In addition, fitting the model considering cell proliferation (and its precursors) alone resulted in a substantially lower log likelihood than fitting the model with fibrosis (and its precursors) alone. This suggests that the processes leading to a change in the alveolar air:blood barrier lead to tumors through changes related to, or correlated with, those that also induce fibrosis, and that there may not be a separate pathway by which changes in the air:blood barrier lead to pre-neoplastic cell proliferation. Because of this last result, the overall likelihood approach did not change the likelihood component (i.e., reflected by the value of -42.731 in Table 4) associated with cell proliferation (BrdU) – that component could be maximized separately from the single pathway leading to the prediction of tumor rates through prediction of the extra risk of fibrosis.

Figures 3 through 7 show the modeled data and the maximum likelihood estimates of the dose-response relationships. In all cases, the x-axis shows lung burden (in m^2 of particle surface area/g lung); the sequence of stages leading from lung burden to the endpoint in question has been “stepped through” to obtain the dose-response curves shown. For example, in Figure 4, LDH is shown as a function of lung burden, where equation 3 has been applied (to get normalized LDH predictions) using the normalized PMN predictions of equation 2, which gives normalized PMN values as a function of lung burden. In all of these figures, the parameters corresponding to the overall maximum likelihood approach have been used (Table 6). Although the fitted curves do not fully predict the data, this is not surprising; in light of the wide variability of the input data for some endpoints (e.g., BrdU), even after normalization, it would be impossible to fit the data perfectly with a monotonic curve. In addition, the apparent discrepancies in the low-dose tumor data vs. fitted line reflect differences of tumor incidence of <3%. Other issues related to fit are addressed in the discussion.

One interesting observation is that since tumor rates are made to explicitly depend on the extra risk of fibrosis, the predicted dose-response curve for the probability of tumors as a function of lung burden plateaus at about 0.17 to 0.18 for lung burdens approaching $1.5 \text{ m}^2 \text{ TiO}_2/\text{g lung}$. That is because the fibrosis extra risk approaches its maximum of 1 at those lung burden values. The plateauing of a tumor response (at a value less than 1) is not something that would be predicted if one modeled lung cancer

rates as a function of lung burden directly. A BMD₁₀ (the dose corresponding to a 10% extra risk of lung cancer) can be estimated from the curve in Figure 7 to be about 0.534 m² TiO₂/g lung.

In order to convert this dose measure to a concentration in air, we used the ratios in Dankovic et al. (2007) between the lung burden (in m²/g lung, for a human exposed for a 45-year working lifetime) and the air concentration, for fine and ultrafine particles. Dankovic et al. used two different models to calculate the air concentration, the CIIT/RIVM Multi-Path Model of Particle Deposition (MPPD) software and a lung interstitialization/sequestration model. While the conversions could be conducted using the same models, using the ratios of the results allows a more direct comparison with the Dankovic et al. (2007) results. Using the ratios obtained from comparison of the results of Dankovic et al. for the Bayesian model averaging using the MPPD model from Dankovic et al., the BMD₁₀ of 0.534 m² TiO₂/g lung corresponds to a 45-year working lifetime exposure to 76 mg/m³ for fine particles, and 8.6 mg/m³ for ultrafine particles. Similarly, the concentration corresponding to a 1/1000 risk (a value commonly used for occupational risk assessment) for a 45-year working lifetime exposure is 3.8 mg/m³ for fine particles, and 0.44 mg/m³ for ultrafine particles. Note that this extrapolation is based directly on the data, and does not include any assumption about linearity or lack thereof.

4.0 DISCUSSION

The purpose of this project was to use data on effect biomarkers (precursor endpoints) quantitatively, to inform the dose-response evaluation and quantitative estimate of cancer risk. In this proof-of-concept analysis, we successfully used a series of linked “cause-effect” functions, fit using an overall likelihood approach, to describe the relationship between successive key events and the ultimate tumor response. This approach has the advantage of estimating the cancer risk in a way that incorporates MOA data, but is not specifically limited to a linear or nonlinear (uncertainty factor-based) extrapolation from a point of departure. In doing so, this study makes use of the early effects biology to evaluate the tumor risk, and so requires less extrapolation from the data, because it explicitly accounts for the pattern of changes in the precursor cause-effect relationships.

The progression of events selected as the basis for the investigation was driven to some extent by the data that were available for analysis. For example, even though ROS are thought to play a major role in inflammation, no measure of ROS was included in the model. The only available data on the production of ROS were from an *in vitro* study, and the tissue dosimetry is not sufficiently refined to extrapolate from such studies. Had appropriate *in vivo* ROS measurements been available, the progression might have included, on the one hand, a linkage between lung burden and the endpoint(s) representing ROS production and, on the other hand, linkages between production of ROS and inflammatory cell responses, loss of integrity of lung cells, and cell proliferation. Lacking endpoints considered to be representative of ROS production, the progression of events (Figure 1) included links directly between TiO₂ lung burden and each of the stages, loss of integrity and cell proliferation. Those links were intended as a

means of allowing the analysis to factor in intermediary events such as ROS production that might influence loss of integrity or cell proliferation, on top of the effects that were directly modeled.

As it turned out in this analysis, the links directly between lung burden and loss of integrity (as measured by LDH), and between lung burden and cell proliferation (as measured by BrdU labeling) were found not to be necessary when the primary pathway from lung burden through inflammatory cell proliferation (as measured by PMN), then through loss of integrity to cell proliferation, was included. That is, the sequential likelihood approach employed here rejected the need (in terms of fit to these data) to include such links; as shown in the Results section, the parameter values corresponding to those links could be set to zero without impact on the likelihood. When the relationships between the endpoints are represented as indicated in this analysis, the effect of TiO₂ lung burden on the proliferation of lung cells, as well as on fibrosis and ultimately lung tumors, appears to be explainable through the pathway that includes inflammation and loss of integrity. These observations are conditional on the constraints within which the analysis was carried out, e.g., conditional on the fact that all the cause-effect relationships were modeled with a power function. It is also always worth keeping in mind that the proposed explanatory variables in equations 3, 4, and 6 would be correlated because they all ultimately depend on (are predicted from) lung burden.

Moreover, the pattern of dose-responses observed for the selected precursors (Figures 2a and 2b) supports the idea of a progression or cascade of events as shown in Figure 1. The PMN response was observed to be increased at lower lung burdens than the LDH response, and the LDH response was increased at lower lung burdens than the alveolar BrdU index of cell proliferation. Similarly, rates of fibrosis were observed to increase before the rates of tumors, and both of those were increased at about the same lung burden levels as those that increased cell proliferation. Although not shown here, the other endpoints that might have been selected as representatives of the stages of the progression (e.g., macrophages for the inflammatory response, GGT for the loss of integrity, or BrdU index for bronchiolar cells for cell proliferation) also tended to support the sequence shown in Figure 1.

The assumed relationships between pairs of continuous endpoints/precursors were fixed via preliminary examination of the general pattern of dose-response. Such a pre-selection of a dose-response function (the power function) appeared to be reasonable (and the power function is fairly flexible in fitting different dose-response patterns), but it is an expedient approach. For this analysis the power model appeared to provide reasonable fit, and our focus was developing and implementing a procedure that can be used for cross-study integration of various endpoints thought to be important for characterizing a cascade of effects leading to a measureable endpoint of clinical concern. Thus, we have not rejected the selected models or their fits to the data due to large chi-squared goodness-of-fit statistics.¹ A more rigorous procedure that investigates alternative dose-

¹ Likelihood ratio test statistics can be determined based on the log-likelihoods shown in Table 4. The saturated model for each endpoint had 36, 36, 24, 20, and 20 parameters for the PMN, LDH, BrdU, fibrosis, and tumor data sets, respectively, compared to 2, 2, 2, 4, and 2 parameters for the corresponding

response functions would be consistent with current approaches for dose-response modeling to support risk assessments and would be an important enhancement if this analysis were intended to be used for regulatory purposes. Nevertheless, the current model selection approach we have used is appropriate for demonstrating the methods for developing a linked functions approach for more fully using biomarker data to inform dose-response. In addition, this analysis did not consider models that included a threshold for any of the precursor events, and so this analysis could not evaluate whether a threshold exists for these events or for tumors. Threshold models could be considered in an expanded search for suitable models, although it should be noted that inclusion of threshold terms in models adds computational difficulties and may be controversial. In any case, extensions of this current investigation would consider a wider range of dose-response functions and extend the likelihood-based approach used here to include model choice as part of the maximization of the likelihood; more elaborate algorithms for likelihood maximization would be needed to accomplish that.

Similarly, model choice for the dichotomous endpoints (fibrosis and tumors) was based on expediency and identification of curves (1-hit for fibrosis and logistic for tumors) with the appropriate underlying shape to fit the data. The fibrosis response rises fairly rapidly, with clear increases at lung burdens of 0.25 and 0.3 in the one study (two data sets – Lee et al. males and females) in which it was measured at relatively high lung burdens. The one other study that reported fibrosis incidence (Muhle et al, 1991) reported only a small increase, but tested much lower lung burdens. In contrast, at the same lung burden doses (0.25 and 0.3) where clear increases in fibrosis incidence were noted, there was no increase in lung tumors in the Lee study, and so a model that could fit an S-shaped curve was needed. As for the continuous data, a more rigorous procedure that investigates alternative dose-response functions would be consistent with current approaches for dose-response modeling in risk assessment. Furthermore, the use of a 1-hit model for the fibrosis data does not imply anything about a specific mechanism; the choice of model function was based on adequate overall dose-response pattern

Future analyses will have to consider how goodness-of-fit determinations can be best performed with endpoints that are linked as shown here. For example, the fits of the model to the LDH data, with PMN as the predictor (explanatory variable), depend not just on the predictions of the LDH observations but also on the predicted PMN values, so it is not as straightforward to determine the number of parameters that are “used” by the LDH model, compared to the case where one could model LDH as a function of lung burden directly. Moreover, as mentioned above, the comparison of the fitted model likelihoods to those for the saturated models is not clearly the best basis for determining how well these models predict data that vary nonmonotonically, when the models themselves are constrained to be monotonic. This is an issue with the “alternative” hypothesis in the goodness-of-fit calculation, one that needs a more complete

fitted models. The resulting p-values for goodness of fit were therefore 0.0009, 0.014, 0.001, 0.0002, 0.061, for the PMN, LDH, BrdU, fibrosis, and tumor models, respectively, based on the sequentially maximized model likelihoods. We have not emphasized these model fit statistics, for the reasons expressed elsewhere and because it is not clear that the simple likelihood ratio approach is the most statistically appropriate method of testing fit in this case of linked models.

consideration, not just for the proposed approach but for risk assessment that assumes monotonicity in general.

In addition, future analyses could examine other issues related to sensitivity by determining the impact on the overall log-likelihood, LL, and on the components of LL (the LL_j values), of changing the parameters in each of the equations representing the transitions from one stage of the progression to another. Those stages for which the sensitivity is highest are those for which additional data might have the biggest impact on identifying the risk associated with TiO_2 exposure; they are the parameters most important to refine with better estimates – and thus such analyses would inform additional toxicology research needs.

The idea of examining changes in the log-likelihoods in relation to parameter value changes is also related to confidence limit calculations. Though not conducted in this analysis, in theory a profile-likelihood approach could be used to define bounds on risk estimates, i.e., bounds on the lung cancer risk associated with specific values of lung burden, or vice versa (Crump and Howe, 1983). Alternatively, simulation-based approaches, e.g., bootstrapping or Markov chain Monte Carlo (MCMC), could be used to characterize the uncertainty associated with risk-related estimates (Carlin and Louis, 2000). Development of any of those approaches should use the overall likelihood as the basis for inference when lung cancer is the clinical endpoint of concern but the progression to tumors is mediated through a sequence of known or suspected precursors.

An MCMC approach offers other advantages as well. In the current analysis, we have treated variance as a “nuisance” parameter; i.e., we assumed independent and group-specific variance terms for which it was simple to calculate the maximum likelihood estimates. The focus of this investigation was on the dose-response pattern rather than the variance pattern. As an extension to this work, one might be interested in modeling the variances as well as the responses for endpoint ‘l’ (e.g., LDH) as a function of its precursor, endpoint ‘p’ (e.g., PMN). That would allow one to move away from using only the maximum likelihood estimates of the dose-response for ‘p’ as predictors for ‘l’; one could, alternatively, define the likelihood based on the predicted mean and variance for ‘p’ at the lung burdens for which ‘l’ was observed. MCMC techniques would be well suited to provide not only the maximum likelihood estimates of the parameters, but also distributions of likelihoods and parameter estimates as well (Carlin and Louis, 2000).

Another possible extension of this work is to broaden the input data. As noted earlier, the inflammation and tumor data for low-toxicity poorly soluble particles form a consistent dose-response curve (when surface area is the dose metric) (Dankovic et al., 2007). Therefore, the model could be extended by including dose-response data for other low-toxicity poorly soluble particles for which there is lung burden data in the appropriate form, and data on the precursor biomarkers of interest. Such data could also help to fill in gaps, such as the absence of data on ROS for TiO_2 exposure. Meaningful inclusion of such data; however, does require the assumption that non-reactive insoluble particles are all acting via the same basic toxicological mechanisms.

Regardless of the development of the extensions to this work as mentioned above, the product of the current analysis provides a proof of concept for an approach to using biomarker data to provide a MOA-informed analysis that extends the dose-response curve below the range of the tumor data. This approach provides an MoA-based alternative to current default low-dose extrapolation approaches (linear or uncertainty factors), and can be used to improve the mathematical description of noncancer or cancer dose-response relationships in the low-dose region, without the need for a full biologically-based dose-response (BBDR) model.

The current analysis, if enhanced as described above (e.g., inclusion of confidence limits, consideration of multiple dose-response functions and goodness of fit), could provide a rational basis for setting regulatory standards for TiO₂ exposures. If one is interested in the risk of tumor development, the approach shown here provides a way to identify the lung burden associated with a risk level of interest, based on the assumption that lung tumors arise via the progression of precursors as represented in Figure 1. Thus, one can focus on the risk of the endpoint of concern (cancer) while accounting for the dose-response patterns of the precursors. This is in contrast to approaches that attempt to set standards based on changes in the precursors (e.g., a 10% change in the mean for some continuous intermediate endpoint such as PMN levels) estimated in the absence of knowledge about the impacts of such a change on the cancer endpoint of interest. Although comparison with alternative analysis methods does not constitute validation of an approach, it is of interest that the concentration calculated here as being associated with a 1/1000 risk over a 45-year working lifetime exposure for exposure to fine particles, 3.8 mg/m³, is in the range of the concentration calculated by Dankovic et al. (2007) based on tumor data (1.0 – 31 mg/m³). Similarly, the concentration that we calculated as being associated with a 1/1000 risk for exposure to ultrafine particles, 0.44 mg/m³, is within the range of 0.1 to 3.5 mg/m³ estimated by Dankovic et al. (2007).

The idea of a progression of stages through various precursors up to cancer development is not new. The two-stage cancer model (Moolgavkar and Venzon, 1979; Moolgavkar and Knudson, 1981), for example, also hypothesizes a sequence of events, in that case represented by a progression through cell types from normal to intermediate to tumorigenic. The two-stage model has a very rigid structure and is based on rates of transition. Of course, the general two-stage framework does not specify how those rates depend on the level of exposure. Moreover, it differs from the modeling of precursors pursued here in that it depends largely on things that are not measurable (accumulation of “intermediate” cells as well as the transition rates themselves). Rather, those unmeasurables and their relationship to exposure must be inferred from indirect observations; with the rigid two-stage structure, estimates of the important parameters of the model can (sometimes) be obtained (given other assumptions about exposure dependency). For our analysis, we are using a less rigid structure (allowing the empirical data to suggest the inter-relationships among the precursors and between the precursors and the cancer incidence rates), and relying on measurable quantities (precursor observations) to estimate parameters of the relationships. Thus, one important difference relates to what data are considered useful for a risk assessment. The emphasis here is on

collecting (and using) measurable, relevant observations, with the relationships among those observations estimated by some flexible and, frankly, not-so-biologically based dose-response equations. In contrast, the two-stage model defines the model structure (to some degree biologically based) and then tries to infer parameter values for that structure using whatever data are best suited, which is often the severest limitation. The empirical, “data driven” approach of the approach described here appears to be appropriate for the analysis of TiO₂ lung cancer prediction; a fuller biologically based set of relationships among the precursors and lung cancer may never become available but, in contrast, measurement of the precursors of interest appears to be relatively straightforward. Development of this approach, therefore, aims to maximize the use of early effect data to inform dose-response behavior for a clinically relevant endpoint for risk assessment. This proposed approach continues the movement toward increasing biology-based decision-making, and provides an empirical method that can enhance assessments for the vast majority of chemicals for which data are inadequate to derive a full biologically-based dose-response model.

Thus, this paper has exhibited an approach for deriving an empirical relationship between lung burden and cancer risk that can be used to set exposure limits and that explicitly considers the effect of precursor biomarker effects on the cancer incidence in rats. Based on this empirical relationship, we estimated a benchmark “dose” level associated with a cancer risk, and extrapolated that lung burden dose to an air concentration under occupational exposure conditions. Similar extrapolations could be done for other exposure scenarios. Application of appropriate uncertainty factors to values estimated from a more complete analysis would yield an estimate that could be used for setting occupational exposure limits.

ACKNOWLEDGEMENTS

This work was funded by P.O. 200-2004-F-10108 from NIOSH. The authors wish to thank Chris Sofge, Eileen Kuempel, and David Dankovic for useful conversations and sharing of data, and Melissa Korhman for technical assistance. However, the text has not been through NIOSH clearance, and therefore reflects the opinions of the authors, and not necessarily that of any NIOSH employees.

REFERENCES

- Boffetta, P., et al., 2001. Exposure to titanium dioxide and risk of lung cancer in a population-based study from Montreal. *Scand. J. Work Environ. Health.* 27, 227-232.
- Boffetta, P., et al., 2004. Mortality among workers employed in the titanium dioxide production industry in Europe. *Cancer Cause. Control.* 15, 697-706.
- Carlin, B.P., Louis, T.A., 2000. Bayes and empirical Bayes methods for data analysis. CRC Press, Boca Raton, Florida.
- Chen, J.L., Fayerweather, W.E., 1988. Epidemiologic study of workers exposed to titanium dioxide. *J. Occup. Med.* 30, 937-942.
- Crump, K.S., Howe, R.B., 1983. Review of methods for calculating confidence limits in low dose extrapolation. In: Clayson, D.B., Krewski, D.R., Munroe, I.C., (Eds.). *Technological Risk Assessment.* CRC Press, Inc. Canada.
- Dankovic, D., Kuempel, E., Wheeler, M., 2007. An approach to risk assessment for TiO₂. *Inhal. Toxicol.* 19, 205-212.
- Delp, M.D., et al., 1998. Effects of aging on cardiac output, regional blood flow, and body composition in Fischer-344 rats. *J. Appl. Physiol.* 85, 1813-1822.
- Driscoll, K.E., 1996. Role of inflammation in the development of rat lung tumors in response to chronic particle exposure. *Inhal. Toxicol.* 8, 139-153.
- Elder, A., et al., 2005. Effects of subchronically inhaled carbon black in three species. I. Retention kinetics, lung inflammation, and histopathology. *Toxicol. Sci.* 88, 614-629.
- Fryzek, J.P., et al., 2003. A Cohort mortality study among titanium dioxide manufacturing workers in the United States. *J. Occup. Environ. Med.* 45, 400-409.
- Haber LT, et al., 2010. [A method for biomarker validation and biomarker-dose response: A case study with a bayesian network model for benzene.](http://www.tera.org/Publications/Publications.html#H) Available at <http://www.tera.org/Publications/Publications.html#H>.
- Hack, C.E., et al., 2010. A bayesian network model for biomarker-based dose response. *Risk. Anal.* 30, 1037-51.
- Heinrich, U., et al., 1995. Chronic irritation exposure of Wistar rats and two different strains of mice to diesel engine exhaust, carbon black, and titanium dioxide. *Inhal. Toxicol.* 7, 533-556.

Hubbard, A.K., et al., 2002. Activation of NF- κ B-dependent gene expression by silica in lungs of luciferase reporter mice. *Am. J. Physiol. Lung Cell. Mol. Physiol.* 282, L968-L975.

International Agency for Research on Cancer (IARC), 1989. IARC monographs on the evaluation of carcinogenic risks to humans: some organic solvents, resin monomers and related compounds, pigments and occupational exposures in paint manufacture and painting. Lyon, France: World Health Organization, International Agency for Research on Cancer, Vol. 47.

International Life Sciences Institute (ILSI), 2000. The relevance of the rat lung response to particle overload for human risk assessment: A workshop consensus report. *Inhal. Toxicol.* 12, 1-17.

Larsen, R.J., Marx, M.L., 2000. An introduction to mathematical statistics and its applications, third ed. Prentice Hall, New York. p. 282.

Lee, K.P., Trochimowicz, H.J., Reinhardt, C.F., 1985. Pulmonary response of rats exposed to titanium dioxide (TiO₂) by inhalation for two years. *Toxicol. Appl. Pharmacol.* 79, 179-192.

Lison, D., et al., 1997. Influence of particle surface area on the toxicity of insoluble manganese dioxide dusts. *Arch. Toxicol.* 71, 725-729.

Maier, A., Savage, R.E., Haber, L.T., 2004. Linking exposure to effect: Are biomarker spectra providing a clearer vision for risk assessment? *J. Toxicol. Env. Heal A.* 67, 687-695.

Moolgavkar, S.H., Venzon, D.J., 1979. Two-event model for carcinogenesis: Incidence curves for childhood and adult tumors. *Math. Biosci.* 47, 55-77.

Moolgavkar, S.H., Knudson, A.G., 1981. Mutation and cancer: A model for human carcinogenesis. *J. Natl. Cancer I.* 66, 1037-1052.

Moss, O.R., Wong, V.A., 2006. When nanoparticles get in the way: Impact of projected area on in vivo and in vitro macrophage function. *Inhal. Toxicol.* 18, 711-716.

Muhle, H., et al., 1991. Pulmonary response to toner upon chronic inhalation exposure in rats. *Fund. Appl. Toxicol.* 17, 280-299.

National Academy of Science, National Research Council (NAS/NRC), 1989. Report of the oversight committee. In: *Biologic markers in reproductive toxicology*. Washington, DC: National Academy of Sciences, National Research Council, National Academy Press.

National Academy of Science, National Research Council (NAS/NRC), 2007. Toxicity testing in the 21st century: A Vision and strategy. Committee on Toxicity Testing and Assessment of Environmental Agents. Washington, DC: National Academy of Science, National Research Council, National Academy Press.

National Institute for Occupational Safety and Health (NIOSH). 2005. NIOSH Current intelligence bulletin: Evaluation of health hazard and recommendations for occupational exposure to titanium dioxide. DRAFT. Cincinnati, OH: U.S. Department of Health and Human Services.

Oberdorster, G., et al., 1994. Correlation between particle size, *in vivo* particle persistence, and lung injury. Environ. Health Persp. 102, 173-179.

Oberdorster, G., et al., 1996. Ultrafine particles as a potential environmental health hazard. Chest 109, 68s-69s.

FIGURE LEGENDS

Figure 1. Pathophysiological progression for lung tumors in rats exposed to TiO₂. Solid lines reflect well-characterized effect relationships, the dashed line reflects a hypothesized relationship, and the dotted lines reflect hypothesized relationships for which data were not available.

Figure 2. Dose-response data for all continuous (2a) and quantal (2b) data used in the modeling. Each endpoint is shown by a different symbol.

Figure 3. PMN vs. Lung Burden - observed data and results predicted using Eq. 2. Each study is shown as a different symbol. CIIT pig – CIIT pigment study, Bermudez (2002); CIIT ult – CIIT ultrafine study, Bermudez (2004); Ferin et al. (1992); Henderson et al. (1995); Ma Hock et al. (2008).

Figure 4. LDH vs. Lung Burden - observed data and results predicted using Eqs. 2 and 3. Each study is shown as a different symbol. Studies as in Figure 3.

Figure 5. Alveolar Cell BrdU Index vs. Lung Burden - observed data and results predicted using Eqs. 2, 3 and 4. Each study is shown as a different symbol. Studies as in Figure 3.

Figure 6. Fibrosis vs. Lung Burden - observed data and results predicted using Eqs. 2, 3, 4, and 5. The three curves have a common slope but study specific intercepts. Each study is shown as a different symbol, with separate symbols and intercepts for the male and female rats in the Lee et al. (1985) study.

Figure 7. Lung Tumor vs. Lung Burden - observed data and results predicted using Eqs. 2, 3, 4, 5, and 6

Table 1. Summary of Exposure and Response Data for Studies and Endpoints Included in the Analysis

Study	Experimental Data	Exposure Levels (mg/m ³)	Lung Burdens (m ² /g lung)	Neutrophils ^a (%)			PMN (/mL)			LDH (U/mL)			Alveolar Cells (% BrdU Labeling Index)			Fibrosis		Tumors ^b	
				N	Mean	SD	N	Mean	SD	N	Mean	SD	N	Mean	SD	N	#Affected	N	#Affected
Muhle et al. (1991)	Fine: 6 hr/d, 5 d/w, 24 mo	0	0	-	--	--	-	--	--	-	--	--	-	--	--	90	1	100	3
	F344, Male and Female	5	0.015	-	--	--	-	--	--	-	--	--	-	--	--	90	5	100	2
Lee et al. (1985)	Fine: 6 hr/d, 5 d/w, 24 mo	0	0	-	--	--	-	--	--	-	--	--	-	--	--	79	11	79	2
	CD, Male	10	0.032	-	--	--	-	--	--	-	--	--	-	--	--	71	7	71	1
		50	0.18	-	--	--	-	--	--	-	--	--	-	--	--	75	49	75	1
		250	1.2	-	--	--	-	--	--	-	--	--	-	--	--	77	76	77	12
	CD, Female	0	0	-	--	--	-	--	--	-	--	--	-	--	--	77	3	77	0
		10	0.069	-	--	--	-	--	--	-	--	--	-	--	--	75	4	75	0
		50	0.28	-	--	--	-	--	--	-	--	--	-	--	--	74	41	74	0
	250	1.2	-	--	--	-	--	--	-	--	--	-	--	--	74	73	74	13	
Heinrich et al. (1995)	Ultrafine: 24 months	0	0	-	--	--	-	--	--	-	--	--	-	--	--	-	--	217	1

	Wistar, Female	10	1.3	-	--	--	-	--	--	-	--	--	-	--	--	-	--	100	19
Ferín et al. (1992)	Fine and Ultrafine: 6 hr/d, 5 d/w, 12 wk	0	0	-	--	--	6	6.80E-6	3.00E-6	-	--	--	-	--	--	-	--	--	--
	F344, Male	23.5	0.17	-	--	--	6	8.74E-4	1.92E-4	-	--	--	-	--	--	-	--	--	--
		23	0.028	-	--	--	6	4.03E-5	3.10E-5	-	--	--	-	--	--	-	--	--	--
Henderson et al. (1995)	Fine: 6h/d, 5d/w, 4 wk	0	0	-	--	--	6	2.60E+3	2.69E+3	6	0.49	0.049	-	--	--	--	--	--	--
	F344, Female	0.1	0.000029	-	--	--	6	3.70E+3	9.06E+3	6	0.41	0.098	-	--	--	--	--	--	--
		1	0.00048	-	--	--	6	2.30E+3	5.63E+3	6	0.44	0.049	-	--	--	--	--	--	--
		10	0.0029	-	--	--	-	--	--	6	0.55	0.073	-	--	--	--	--	--	
Ma-Hock et al. (2008)	Ultrafine: 6 hr/d, 5 d	0	0	-	--	--	5	0.62	0.84	5	0.31	0.060	5	4.27	1.52	--	--	--	--
	Wistar	2	0.0074	-	--	--	5	0.91	0.6	5	0.25	0.360	6	4.99	3.02	--	--	--	--
		10	0.034	-	--	--	5	16.03	5.05	5	0.37	0.290	6	5.27	1.19	--	--	--	--
		50	0.1	-	--	--	5	133.15	56.177	5	1.07	0.450	6	7.28	1.11	--	--	--	--
Driscoll et al. (1991)	Fine: 6 hr/d, 5 d	0	0	-	--	--	-	--	--	5	46	26.833	-	--	--	--	--	--	--
	F344, Male	50	0.0076	-	--	--	-	--	--	5	34	6.708	-	--	--	--	--	--	--
Bermudez (2002)	Fine: 6hr/d,	0	0	5	0.2	0.450	-	--	--	5	23.2	11.367	5	7.25	1.635	--	--	--	--

	5d/w, 13 wk																		
	F344, Female	10	0.015	5	2.7	1.151	-	--	--	5	15.8	5.119	5	5.54	1.214	--	--	--	--
		50	0.095	5	66.3	12.423	-	--	--	5	92.2	17.196	5	8.19	0.562	--	--	--	--
		250	0.25	5	82.9	5.650	-	--	--	5	279.6	16.682	5	9.81	2.599	--	--	--	--
Bermudez (2004)	Ultrafine: 6hr/d, 5d/w, 13 wk	0	0	5	0.4	0.418	-	--	--	5	24.6	2.074	5	4.53	1.777	--	--	--	--
	F344, Female	0.5	0.0058	5	0.5	0.354	-	--	--	5	25.8	1.924	5	6.23	2.416	--	--	--	--
		2	0.023	5	6.5	4.228	-	--	--	5	29.2	6.611	5	7.81	1.223	--	--	--	--
		10	0.15	5	64.8	5.346	-	--	--	5	122.2	18.580	5	12.18	2.533	--	--	--	--

Abbreviations: PMN = polymorphonuclear lymphocytes; LDH = lactate dehydrogenase

^a Neutrophil data were combined with PMN data after normalization.

^b The following tumor types were observed and included: Muhle et al., 1991 – lung adenoma and adenocarcinoma; Lee et al., 1985 – bronchioloalveolar adenoma; Heinrich et al., 1995 – adenomas and adenocarcinomas. Squamous cell carcinomas and keratinizing cysts were not included for any study.

Table 2. Studies and Endpoints Included in the Analysis

Study	Rat Strain/Sex	TiO₂ Characteristics	Specific Surface Area, m²/g (source)	Other Basis for Lung Burden Calculation	Endpoints Included in Analysis
Lee et al. (1985)	CD/M	Fine	4.99 (Driscoll, 1996)	NIOSH (2005)	Fibrosis, Tumors
Lee et al. (1985)	CD/F	Fine	4.99 (Driscoll, 1996)	NIOSH (2005)	Fibrosis, Tumors
Driscoll et al. (1991)	F344/M	Fine	4.99 (Driscoll, 1996)	Lung wt/body wt ratio from Delp et al. (1998)	LDH
Muhle et al. (1991)	F344/M&F	Fine, Rutile	4.99 (Driscoll, 1996)	NIOSH (2005)	Fibrosis, Tumors
Ferin et al. (1992)	F344/M	Fine Ultrafine	6.5 50	Lung wt/body wt ratio from Delp et al. (1998)	PMN
Heinrich et al. (1995)	Wistar/F	Ultrafine	48 (reported)	NIOSH (2005)	Tumors
Henderson et al. (1995)	F344/F	Fine	6.68 (NIOSH)	µg/g lung reported	PMN, LDH
Bermudez et al. (2002)	F344/F	Pigment (fine)	8.46 (reported)	Individual µg/lung could be calculated from technical reports	PMN ^a , LDH, BrdU
Bermudez et al. (2004)	F344/F	Ultrafine	49.71 (reported)	Individual µg/lung could be calculated from technical reports	PMN ^a , LDH, BrdU

Ma-Hock et al. (2008)	Wistar/M	Nano (ultrafine)	51.1 (reported)	Reported mean μg $\text{TiO}_2/\text{g lung}$	PMN, LDH, BrdU
-----------------------------	----------	------------------	--------------------	--	-------------------

^aMeasurements of neutrophils in this study were equated to measurements of PMNs (when normalized).

Table 3. Endpoints with Data in Selected Studies, by Type of Event

Type of Event	Endpoints Reported
Inflammatory response	BALF measurements of total cells, neutrophils, PMN , macrophages, lymphocytes
Loss of integrity of the alveolar blood:air barrier	NAG, ALKP, GGT, LDH , protein
Cell proliferation	BrdU labeling index in bronchiolar cells, BrdU labeling index in alveolar cells , BrdU labeling index in parenchymal cells
Fibrosis	Fibrosis
Tumor	Bronchioloalveolar adenoma, SCC, total lung tumors

Endpoints used in the modeling for each type of event are in bold. Bronchioloalveolar adenoma was selected for the Lee et al. (1985) study; total lung tumors was selected for the Heinrich et al. (1995) study (excluding keratinizing cysts) and the Muhle et al. (1991) study.

Abbreviations: ALKP = alkaline phosphatase; BALF = bronchoalveolar lavage fluid; BrdU = bromodeoxyuridine; GGT = γ -glutamyl transpeptidase; LDH = lactate dehydrogenase; NAG = *N*-acetyl- β -D-glucosaminidase; PMN = polymorphonuclear lymphocytes; SCC = squamous cell carcinoma

Table 4. Maximum Likelihood Results: Baseline, Sequential Maximization, and Overall Maximization

Predicted endpoint:	Baseline Log-Likelihoods	Sequentially Maximized Log-Likelihoods	Maximization of Overall Log-Likelihood
PMN	-174.488	-207.270	-207.316
LDH	-79.958	-107.289	-107.378
BrdU	-22.536	-42.731	-42.731
Fibrosis	-217.598	-230.675	-230.253
Tumors	-165.884	-174.715	-174.554
Sum (Overall)	-660.464	-762.680	-762.233

Table 5. Maximum Likelihood Estimates for Model Parameters from the Sequential Fitting Procedure

Predicted endpoint	Text Equation Number	Parameter Values			
PMN	2	$\alpha_1 =$ 2826.211	$\beta_1 =$ 1.524695		
LDH	3	$\alpha_2 =$ 0.109059	$\beta_2 =$ 0.910743	$\gamma_2 = 0$	$\delta_2 = --^a$
BrdU	4	$\alpha_3 =$ 0.621814	$\beta_3 =$ 0.188645	$\gamma_3 = 0$	$\delta_3 = --^a$
Fibrosis	5	$\eta(1) =$ 0.022597	$\eta(2) =$ 0.155016	$\eta(3) =$ 0.024936	$\theta =$ 0.030854
Tumors	6	$\phi_0 =$ -4.69946	$\phi_1 =$ 3.092725	$\phi_2 = 0$	

^aWhen γ_2 or γ_3 equals zero, the value of the power (δ_2 or δ_3 , respectively) is immaterial.

Table 6. Maximum Likelihood Estimates for Model Parameters from the Overall Maximum Likelihood Fitting Procedure

Predicted endpoint	Text Equation Number	Parameter Values			
PMN	2	$\alpha_1 =$ 2697.475	$\beta_1 =$ 1.501885		
LDH	3	$\alpha_2 =$ 0.128698	$\beta_2 =$ 0.881975	$\gamma_2 = 0$	$\delta_2 = --^a$
BrdU	4	$\alpha_3 =$ 0.606409	$\beta_3 =$ 0.197698	$\gamma_3 = 0$	$\delta_3 = --^a$
Fibrosis	5	$\eta(1) =$ 0.022832	$\eta(2) =$ 0.15565	$\eta(3) =$ 0.025188	$\theta =$ 0.030184
Tumors	6	$\phi_0 =$ -4.69993	$\phi_1 =$ 3.104775	$\phi_2 = 0$	

^aWhen γ_2 or γ_3 equals zero, the value of the power (δ_2 or δ_3 , respectively) is immaterial.

Figure 1. TiO₂ Tumor Progression

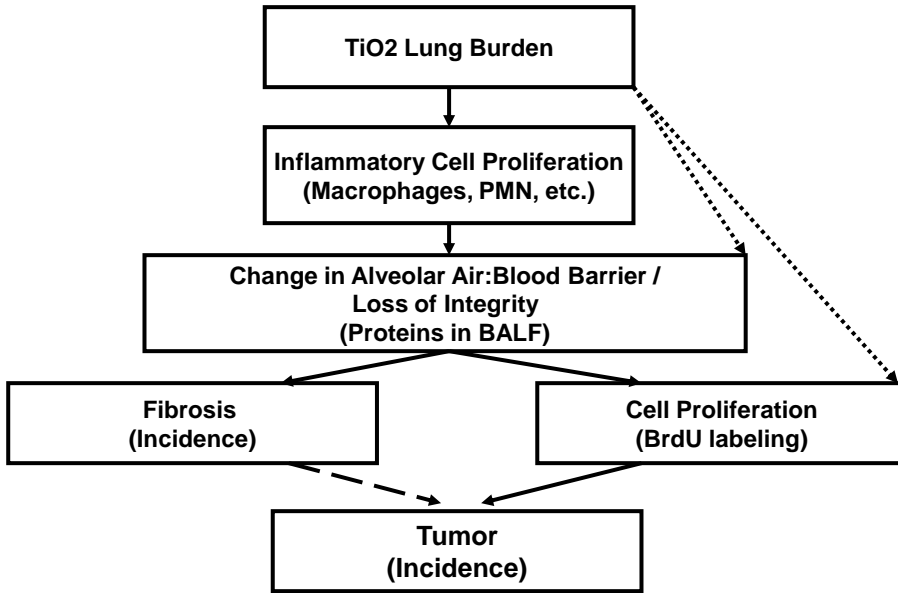


Figure 2a

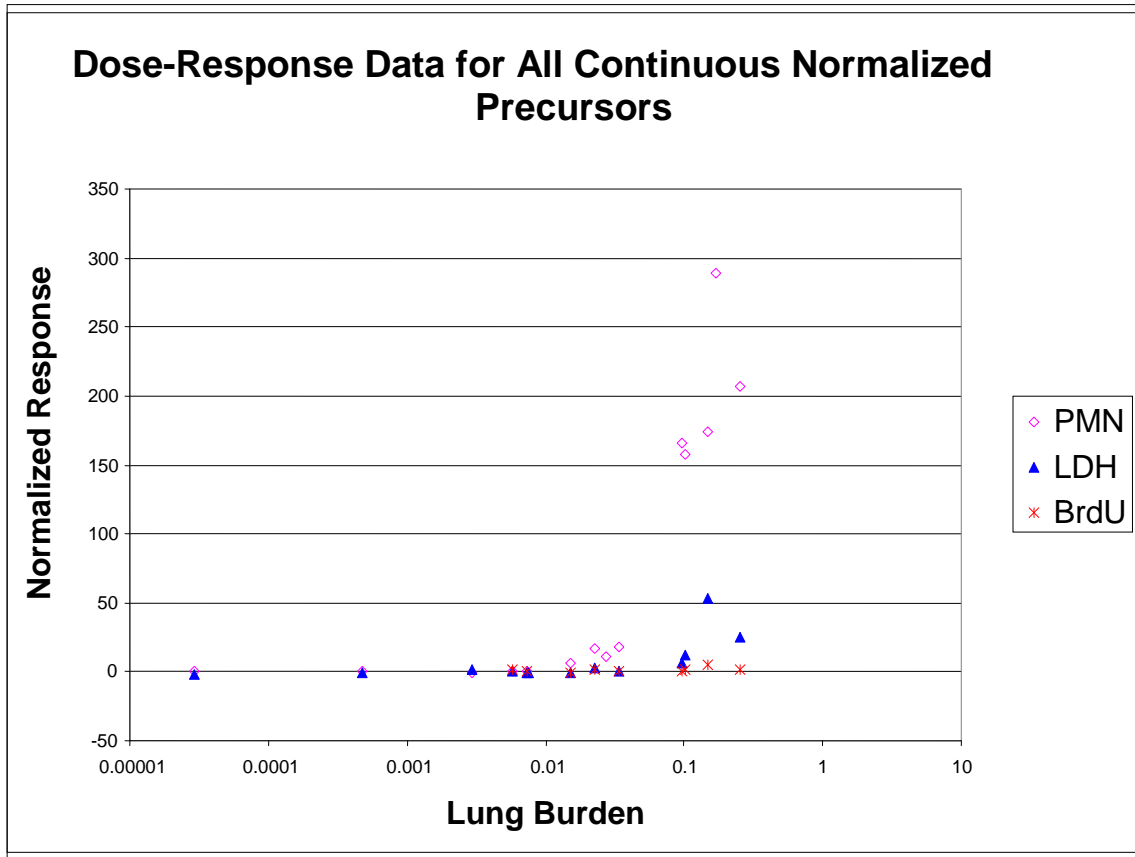


Figure 2b

Dose-Response Data for Fibrosis and Tumors

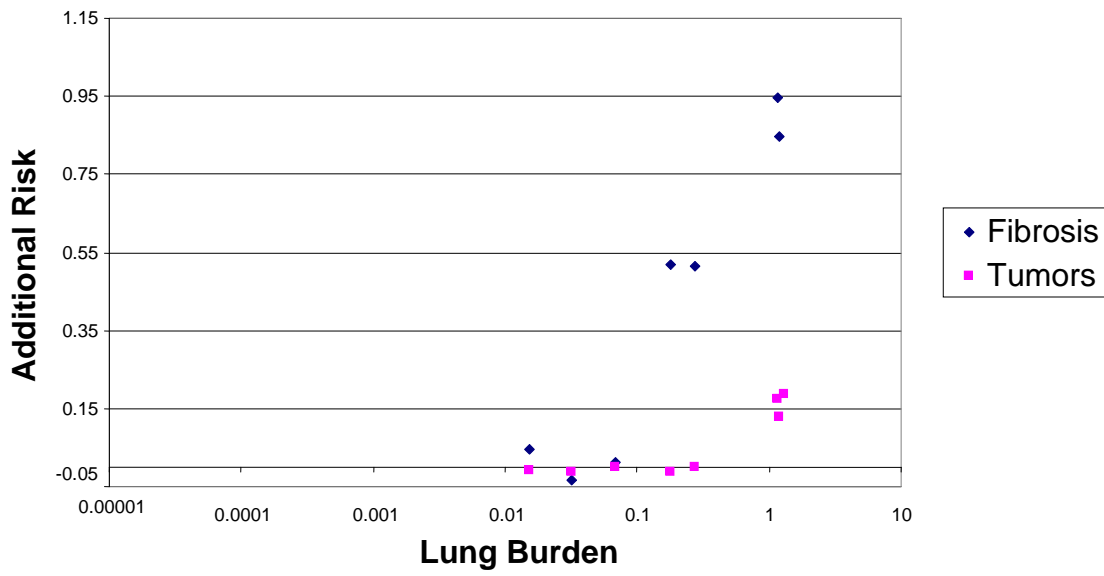


Figure 3. PMN vs Lung Burden

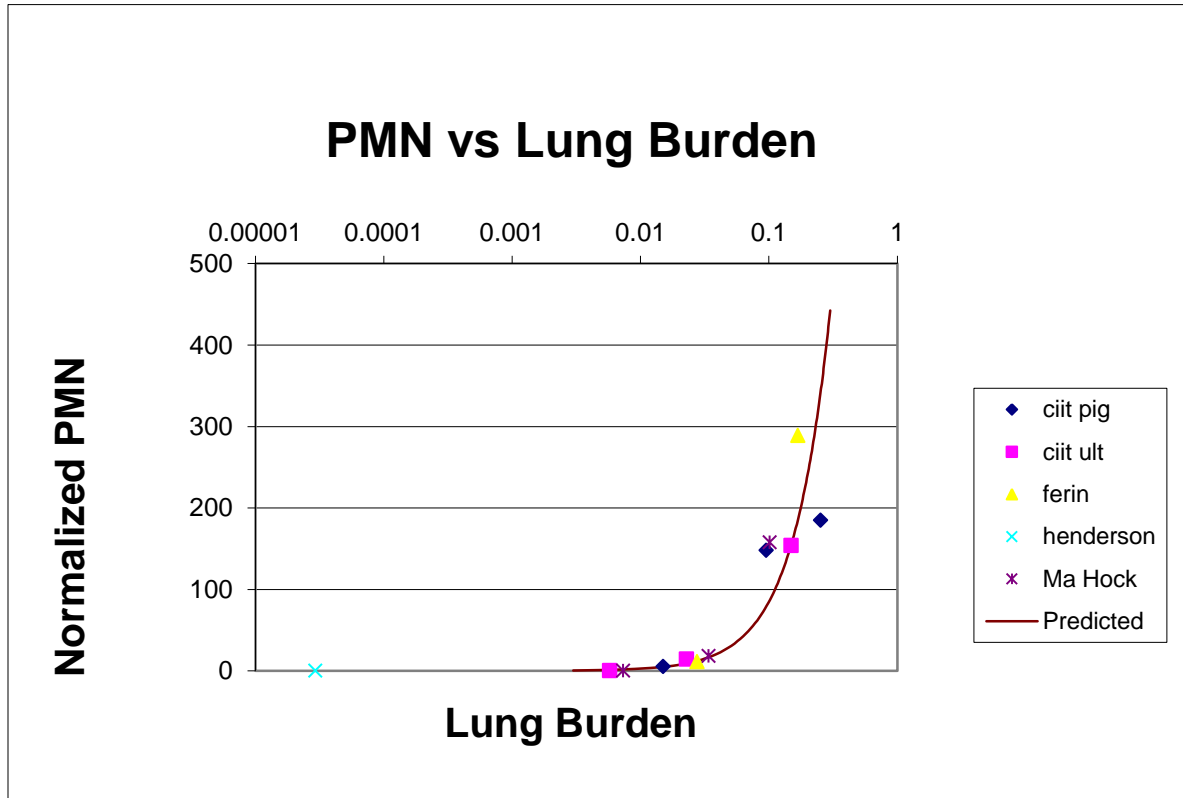


Figure 4. LDH vs Lung Burden

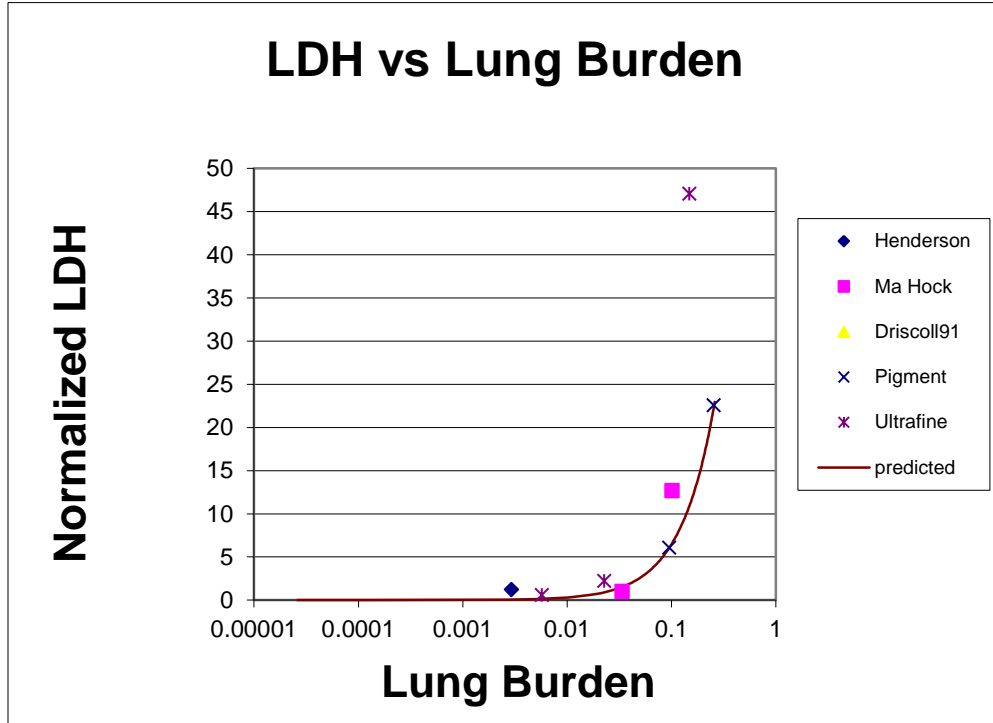


Figure 5. Alveolar Cell BrdU Index vs Lung Burden

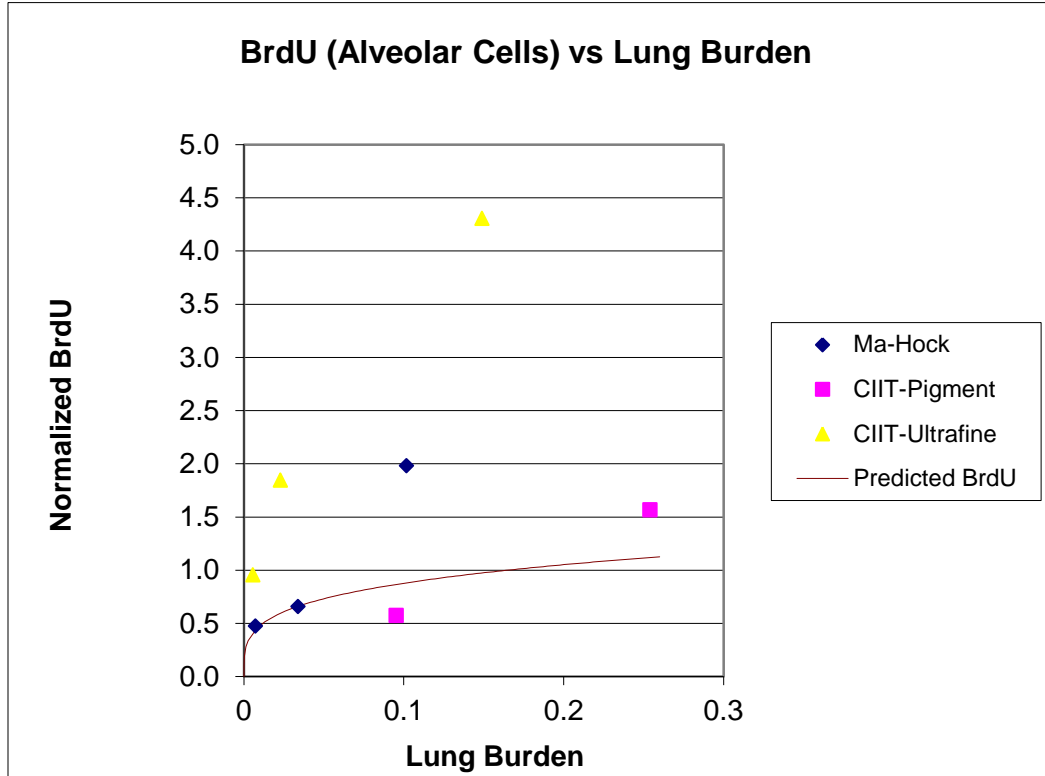


Figure 6. Fibrosis vs Lung Burden

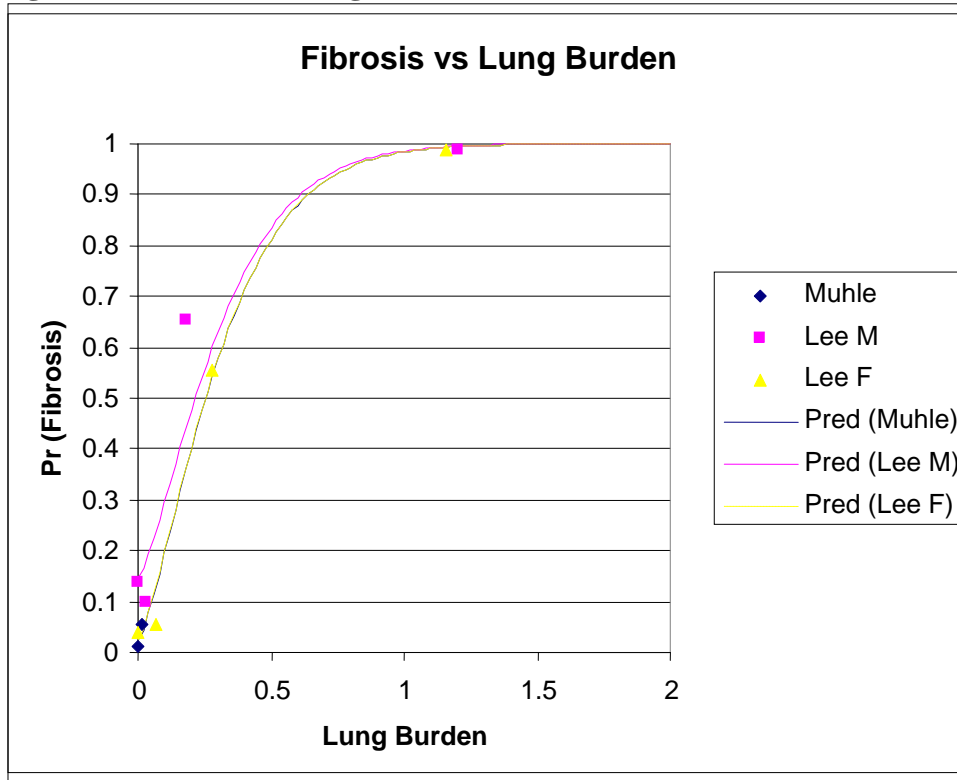


Figure 7. Lung Tumor vs Lung Burden

